J. Chem. Sci. (2022)134:104
https://doi.org/10.1007/s12039-022-02099-1

REGULAR ARTICLE

Effective adsorption of chlorpyrifos pesticides by HKUST-1 metal-organic framework

BHARTI KANGRA[a], ANUSHREE JATRANA[a,*], SHEETAL MAAN[a], SONU CHAUHAN[a] and VINAY KUMAR[b]

[a]Department of Chemistry, Chaudhary Charan Singh Haryana Agricultural University, Hisar, Haryana 125001, India
[b]Department of Physics, Chaudhary Charan Singh Haryana Agricultural University, Hisar, Haryana 125001, India
E-mail: anushree@hau.ac.in; anushreejatrana@gmail.com

MS received 11 May 2022; revised 22 July 2022; accepted 15 August 2022

Abstract. Increased use of pesticides has led to severe environmental and health issues in terrestrial and aquatic ecosystems, and precise removal of pesticides from the environment is of great importance. Therefore, this problem has attracted the attention of researchers toward metal-organic frameworks, which can be used as adsorbents because of their high porosity, large surface area, more active sites, and easy production. In this study, HKUST-1 was synthesized by the solvothermal method. The characterization of this copper-based metal-organic framework (MOF) was done by different techniques, i.e., XRD, FTIR, PSA, FESEM, EDX, and N_2-sorption. HKUST-1 was applied for adsorptive removal of chlorpyrifos, where the correlation between the parameters, such as adsorbent dose, pH, temperature, and contact time, were optimized. Under optimal conditions, the maximum adsorptive capacity for chlorpyrifos was found to be 102 mg/g, and the maximum removal efficiency was recorded as 76%. The results from the present study can be considered important for potential future applications of MOFs, especially to attend environmental issues.

Keywords. Metal-organic framework; HKUST-1; Chlorpyrifos; Adsorption; Environmental pollution.

1. Introduction

Metal-organic frameworks (MOFs) are an interesting class of porous crystalline materials with unique properties, like high specific surface area, tunable pore-size, large porosity, low density, and structural diversity.[1] These outstanding properties make them promising materials for diverse applications, like, gas storage[2] separation, catalysis,[3] drug delivery,[4] sensing,[5] and energy storage.[6] In recent years, MOFs have become a focus of research for various environmental applications. Water pollution due to pesticides is an increasing concern because of their significant threat to the environment, particularly human health. Recent scientific knowledge proposes that environmental pollution due to pesticides is at a dangerous level. Stringent testing standards and permitted pollutant levels make cost-effective water treatment technologies the most extreme need of the hour. Pollution due to pesticides has drawn a lot of attention in recent years, as these chemicals have become an integral part of our agriculture system. Since the onset of the green revolution, extensive agricultural use of agrochemicals has been observed, and approximately 5.2 billion pounds of pesticides are used worldwide every year.[7,8] Pesticides cause health problems like carcinogenesis, mutagenicity, damage to the nervous system, reproduction, infertility, and liver damage.[9]

A study from the Centre for Science and Environment (CSE) recently drew attention to the concentration of pesticides such as organochlorines and organophosphates exceeding the WHO standards in almost all Indian bottled water.[10] Environmental Protection Agency (EPA) reported $>$ 50% water pollution due to the mixing and leaching of chemicals in streams and rivers.[11] Pesticide contamination of surface and

*For correspondence

Supplementary Information: The online version contains supplementary material available at https://doi.org/10.1007/s12039-022-02099-1.

Published online: 05 October 2022

groundwater is a subject of national importance, which force the researchers to further explore their mitigation.

Various methods have been investigated for removing pesticides from an aqueous environment, including oxidation, photocatalytic processes, membrane separation, electrochemical decomposition, and adsorption. Out of these processes, the adsorption method is more convenient due to its low operating cost, wide application range, simple design, no secondary pollution, and easy regeneration of the adsorbent.[12] Therefore, it is critical to developing a high-capacity adsorbent for effective and rapid removal of pesticides from the water *via* adsorption. Porous solids hold a special interest as a sustainable material for adsorptive removal, as the presence of pores facilitates easy adsorption. Due to its specific property to form well-organized structures by molecular building blocks with spatial control over atomic scale, tremendous significance has been given to the field of porous crystalline materials. Over the past few years, an infinite number of solids having metal ions linked to organic moieties have been explored.[13]

Herein we report the synthesis of HKUST-1 by the solvothermal method, which was further explored for adsorptive removal of chlorpyrifos. The adsorption kinetics and isotherm were studied in order to provide information about the mechanisms involving material structure to remove pollutants during water treatment.

2. Experimental

2.1 *Material and method*

Chlorpyrifos (1000 mg/L) pesticide was obtained from residue analysis lab, Entomology Department, College of Agriculture, CCSHAU, Hisar. Trimesic acid was procured from Sigma Aldrich Pvt. Ltd. Copper nitrate trihydrate (AR/ACS), N, N-Dimethyl formamide (AR) were procured from Central Drug House (P) Ltd. Sodium hydroxide pellets (extra pure AR) were supplied by Sisco Research Laboratories Pvt. Ltd. Chlorpyrifos concentrations were determined using the maximum absorbance (at 290 nm) through UV-Vis spectrophotometer, Shimadzu 1900. The calibration curve was plotted for different concentrations of chlorpyrifos, ranging from 20-200 mg/L.

2.2 *Synthesis of HKUST-1*

MOF was synthesized by the solvothermal method, where copper nitrate trihydrate (4.34 g) and trimesic acid (2.4 g) were mixed with dimethyl formamide (DMF), followed by stirring at ambient temperature for half hour. The mixture was then poured into the autoclave and kept inside the oven pre-heated at 120 °C for 18 h. After completion of the reaction, the contents were subjected to filtration, and the residue was dried in an oven, and crushed to achieve the fine powder. Various synthesis steps used to obtain HKUST-1 are represented in Figure S1 (SI). The percent yield was calculated by following the general equation.

$$\text{Percent yield}(\%) = \frac{\text{Actual weight}}{\text{Theoretical weight}} \times 100 \quad (1)$$

2.3 *Characterization*

MOFs were characterized by various techniques like X-ray diffraction (XRD), Fourier transforms infrared spectroscopy (FTIR), Particle size analysis (PSA), BET surface area analyzer, and Field emission scanning electron microscopy (FESEM). The infrared-induced vibrations were recorded on a Thermo Scientific spectrometer (Nicolet-is 50) from 4000 to 400 cm^{-1}, at a scan speed of 4 cm^{-1}. Particle size analysis was carried out by Microtrac particle size analyzer (Nanotrac wave II). The crystal structure of HKUST-1 was studied by Bruker AXS D8 diffractometer in the 2θ range of 20-80°, at a scanning rate of 2° min^{-1}. Quantachrome ASiQwin^{TM} analyzer was used to carry out the adsorption-desorption measurements with vacuum degasification of the sample for 12 h at 120 °C. BET method was used to calculate the specific surface area, DFT method was used to analyze the pore size distribution, and the adsorbed amount of nitrogen was used to assess the pore volume. The surface topography and crystal size of MOF was established by FESEM, using a Quanta 200F microscope with 20 kV of an accelerating voltage. Energy-dispersive X-ray spectrometer (EDX, Oxford Instruments, 51 XMX 1005) coupled with FE-SEM chamber confirmed the elemental composition of MOF.

2.4 *Adsorption experiments*

Batch experiments were carried out for optimization of various reaction parameters, i.e., *pH*, amount of HKUST-1, time, and temperature. The removal efficiency (%) and adsorptive capacity (q_t) of MOF were calculated by using the following equations:

$$\text{Efficiency} = \frac{\text{Initial concenteration} - \text{Final concenteration}}{\text{Initial concenteration}} \tag{2}$$

$$\text{Adsorptive capacity} = \frac{(\text{Initial cocenteration} - \text{Final concenteration}) \times \text{Volume}}{\text{Mass of adsorbent}} \tag{3}$$

2.5 *Study of adsorption isotherms and kinetic modeling*

Non-linear Langmuir and Freundlich isotherms were used to analyze the adsorption isotherm data, by applying their respective equations, 4 & 5:

$$\frac{Ce}{q_e} = \frac{1}{K_L * q_{max}} + \frac{C_e}{q_{max}} \tag{4}$$

$$q_e = K_f * C_e^{1/n} \tag{5}$$

Where C_e is the concentration at equilibrium, q_e is adsorptive capacity at equilibrium, q_{max} is the maximum adsorptive capacity, K_L is the Langmuir constant, K_F is the Freundlich constant, and 1/n is the linearity of adsorption.

The pseudo-first-order and pseudo-second-order equations were used for kinetic modeling, as given by equations 6 & 7.

$$\ln(q_e - q_t) = \ln q_e - \frac{k_1}{2.303} t \tag{6}$$

$$\frac{t}{q_t} = \frac{1}{k2q_e^2} + \frac{t}{q_e} \tag{7}$$

Where, q_e is the adsorptive capacity at equilibrium, q_t is the adsorptive capacity at time t, k_1 and k_2 are the reaction rate constant of pseudo first and second order, t is the time.

3. Results and Discussion

3.1 *Characterization of HKUST-1*

3.1a *FTIR analysis*: FTIR study was conducted to confirm the presence of both inorganic and organic species in the sample (Figure 1). FTIR spectrum showed the presence of a characteristic Cu-O band at 730 cm^{-1}, which indicated the successful formation of metal-ligand coordination.[14] The out-of-plane vibrations of BTC were shown by bands ranging from 600-1300 cm^{-1}. The bands at 1450 and 1649 cm^{-1} correspond to –O-C-O- bonding, while bands at 1373 and 1548 cm^{-1} correspond to stretching of C=C, exhibiting the assimilation of BTC in the MOF.[15] The FTIR spectrum of HKUST-1 after the adsorption study has shown negligible difference from the unused sample (Figure S2, SI), indicating no structural change during adsorption.

3.1b *Particle size and zeta potential analysis*: The determination of HKUST-1 diameter was carried out by using a particle size analyzer. PSA results indicated that the particle size range of HKUST-1 was from 4900 nm to 5300 nm (Figure 2). The zeta potential and polarity values of HKUST-1 at neutral pH were +45.8 (mv) and positive, respectively (Table S1, SI). The zeta potential analysis results indicated that HKUST-1 had a net positive charge on its surface as it represented the zeta potentials of greater than +30 mV.[16]

3.1c *XRD analysis*: XRD analysis was performed to ensure the purity of crystalline phases in HKUST-1 (Figure 3), which exhibited prominent peaks at 2Θ of 5.7, 9.54, 11.7, and 13.07°, corresponding to the regular (002), (022), (222) and (004) planes of HKUST-1. Other peaks at 2Θ of 18.03, 25.9, 29.3, 35.7, and 38.78° corresponded to (044), (355), (555),

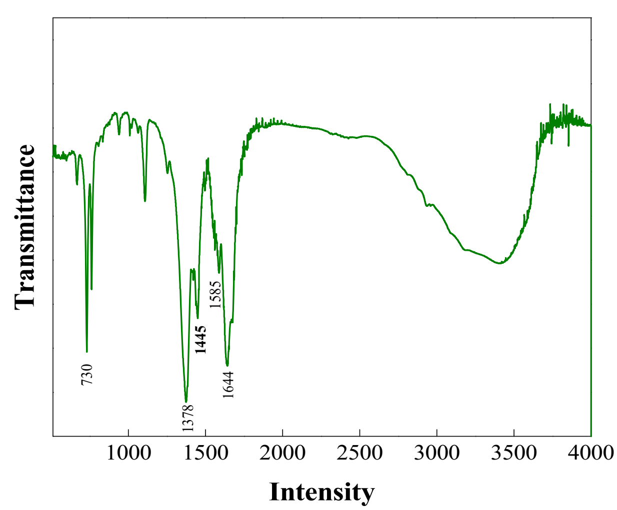

Figure 1. FTIR spectrum of HKUST-1.

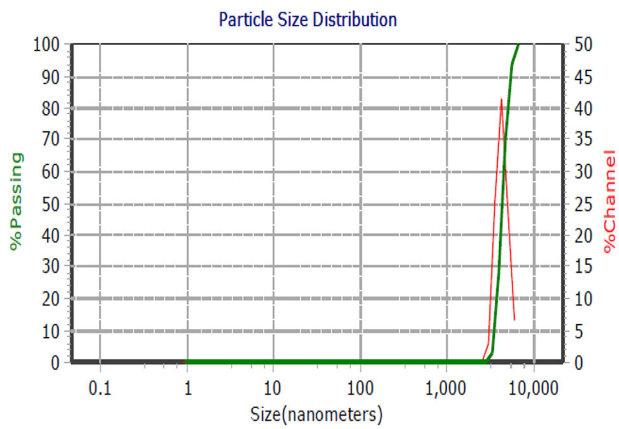

Figure 2. Particle size distribution of HKUST-1.

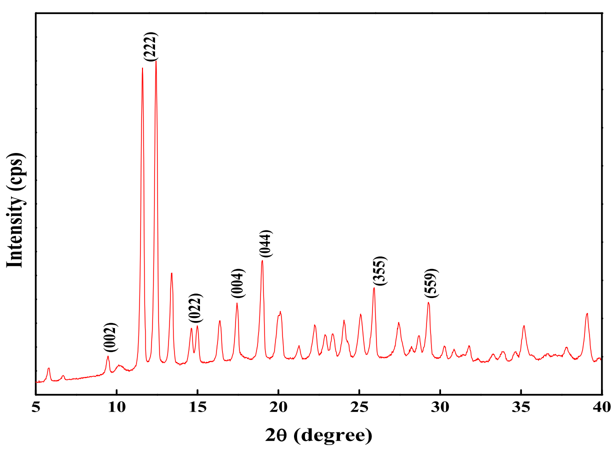

Figure 3. XRD of HKUST-1.

(377), and (559) planes, respectively. XRD pattern clearly establishes that the pure HKUST-1 phase was formed without any second phase.[17]

3.1d *FESEM analysis*: The morphology of HKUST-1 was investigated by FESEM analysis (Figure 4 (a) & (b)). Based on micrographs, it was concluded that the synthesized HKUST-1 produced octahedral crystals with different sizes of 4.9, 5.7, 10.8, and 13.2 μm. These results were comparable with the earlier reports.[18] In EDX results shown in Figure S3 (SI), the elemental composition of HKUST-1 was found to consist of 57.35% at. of C, 34.61% at. of O, and 8.04% at. of Cu.

3.1e *N_2 sorption analysis*: N_2 sorption technique was used to analyze the isotherms and pore size distribution, as presented in Figure 5. The adsorption/desorption isotherm of HKUST-1 was found to be of type I. The isotherm indicated a sudden rise in the adsorbed quantity with an increase in the relative pressure and then saturation, indicating single-layer adsorption of adsorbate over the surface of the adsorbent. These are characteristic features of the microporous materials, which have almost comparable pore sizes to the molecular diameter of the adsorbate resulting in monolayer adsorption.[19,20] The studies also show that the BET surface area is 507.080 m^2/g, and the pore size distribution peak is at 19 Å (Figure S4, SI) with a total micropore volume of about 0.24 cc/g.

3.2 *Adsorption studies*

Batch studies were carried out to study the adsorptive removal of chlorpyrifos. In order to study the effect of pH, chlorpyrifos solution (20 mL) was adjusted to different *pH* of 3, 4, 5, 6, 7, 8, 9. Different amounts of

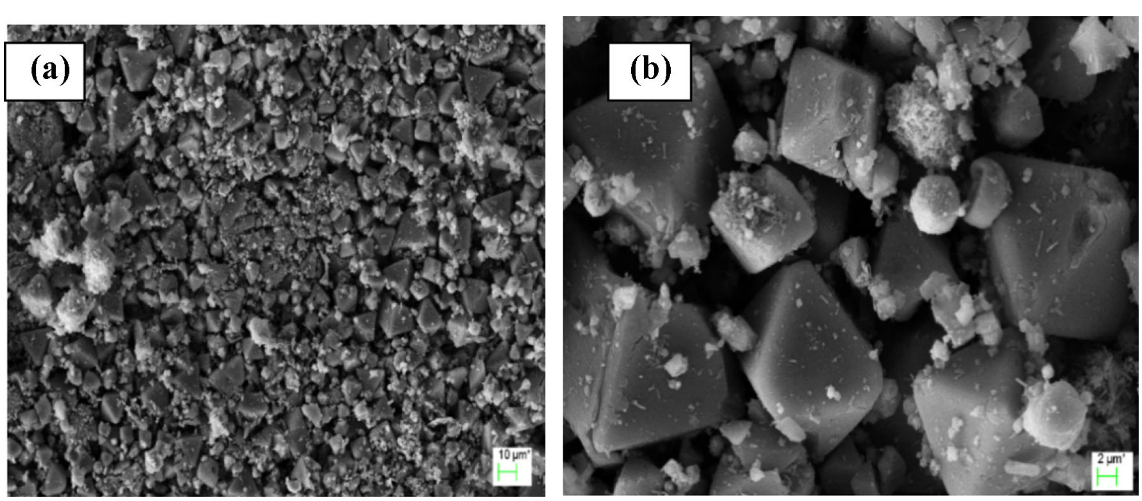

Figure 4. FESEM micrograph at different scales (a) 10 μm (b) 2 μm.

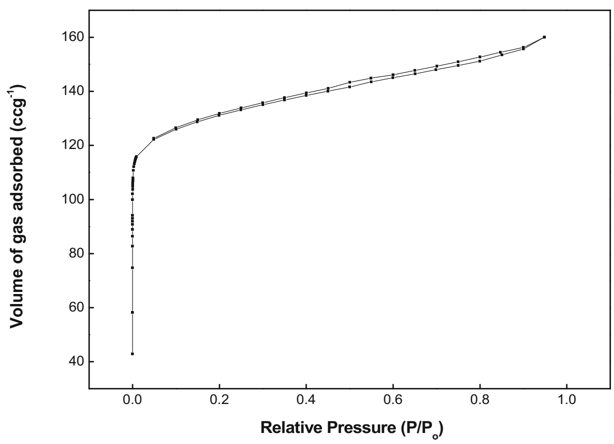

Figure 5. N_2-sorption isotherms of HKUST-1.

HKUST-1, i.e., 10, 20, 30, 40, 50 mg, were added to the chlorpyrifos solution to observe the effect of the amount of HKUST-1. To optimize contact time and temperature, adsorption studies were carried out at different times (10, 20, 30, 40, 50, 60 min) at different temperatures (30 °C, 45 °C, 60 °C). Lastly, the initial pesticide concentration was optimized by taking different concentrations (25, 50, 75, 100, 125, 150 ppm) of the pesticide under other optimized conditions.

3.2a *Effect of pH*: The solution pH is important for the adsorption process, as it has a direct effect on the charge of functional groups of adsorbent. The *pH* of chlorpyrifos solution was optimized from 3 to 9 in order to find the most favourable *pH* value for adsorption. The results revealed that the removal efficiency was increased with an increment in pH and reached maximum removal of 76% at *pH 7*, while further increments in *pH* caused a decrease in removal efficiency. In the case of adsorptive capacity, a maximum value of about 38 mg/g was obtained at *pH* 7 (Figure 6). PSA study revealed that the surface of HKUST-1 had a positive charge at *pH* 7, while literature indicates that chlorpyrifos pesticide carries a negative charge.[21] Therefore, the electrostatic attraction between chlorpyrifos and MOF at neutral *pH* resulted in higher adsorption efficiency.

3.2b *Effect of amount of adsorbent*: The amount of HKUST-1 was optimized by varying its weight from 10 to 50 mg (Figure 7). Results revealed that adsorption increases with an increment in the quantity of HKUST-1 from 10 to 20 mg, while a gradual decrease was observed with the increase from 30 to 50 mg. Therefore 20 mg was taken as an optimized amount with maximum removal of 74%. This decrease in efficiency at a higher amount of

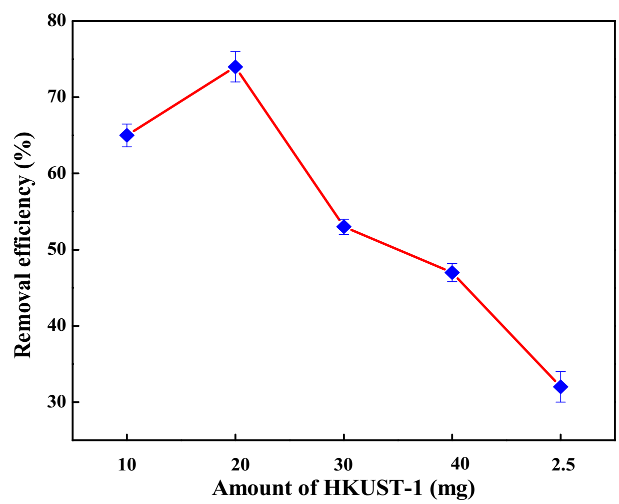

Figure 7. Effect of amount of HKUST-1 on removal efficiency.

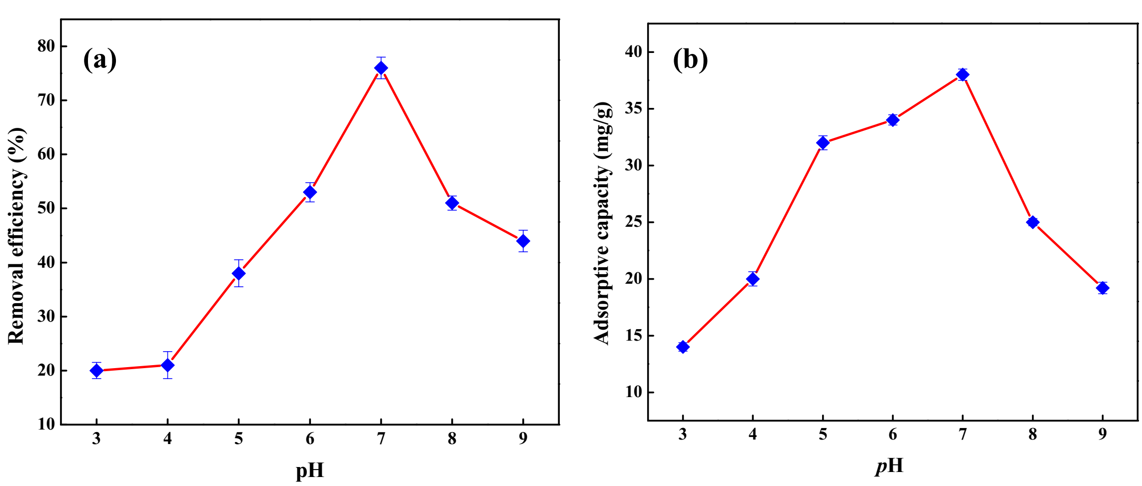

Figure 6. Effect of pH on (a) removal efficiency (b) adsorptive capacity.

HKUST-1 may be related to the blocking of active sites due to agglomeration.[22]

3.2c *Effect of temperature and contact time*: The contact time and temperature were optimized in order to study their simultaneous effect on removal efficiency. For this study, contact time was varied from 10 min to 60 min at different reaction temperatures of 30 °C, 45 °C, and 60 °C. The maximum removal at 30 °C was obtained in 60 min (76%). At 45 °C maximum removal of 79% was achieved in 50 min, while it took 40 min to achieve the maximum removal of 81% at 60 °C. At every rise of temperature by 15 °C there was a decrease of 10 min in equilibrium time, as shown in Figure 8. This is because as the temperature increases, the number of collisions increases, and the rate of reaction becomes fast, resulting in decreased reaction time.[23]

3.2d *Effect of initial concentration of pesticide*: In order to study the effect of initial chlorpyrifos concentration on percent removal, its concentration was varied from 25 mg/L to 150 mg/L. Results indicated that the percent removal is decreased with the increasing concentration of pesticide (Figure 9), and the maximum removal of 76% is observed at 25 mg/L. As the amount of HKUST-1 that we added to the solution is similar at all concentrations, the adsorption sites are limited; therefore, the removal efficiency was decreased at increased concentration. It was also reported the decrease in removal efficiency of HKUST-1 with increasing concentration of lead.[25]

The above discussion shows that the maximum removal efficiency for chlorpyrifos pesticide using HKUST-1 is 76%. This maximum removal efficiency is obtained for pesticide solution of 20 ppm concentration having 7 *p*H added with 20 mg of adsorbent with a contact time of 60 min at 30 °C. Before this, removal of various other organic pollutants using HKUST-1 has been reported, and their removal efficiencies are given in the below Table 1:

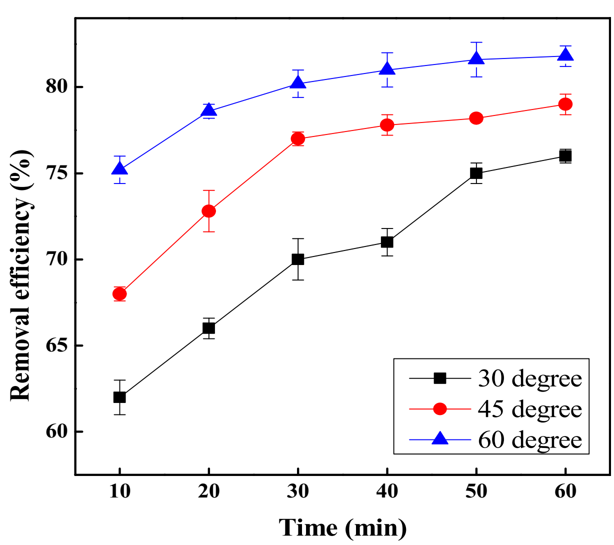

Figure 8. Effect of time and temperature on removal efficiency.

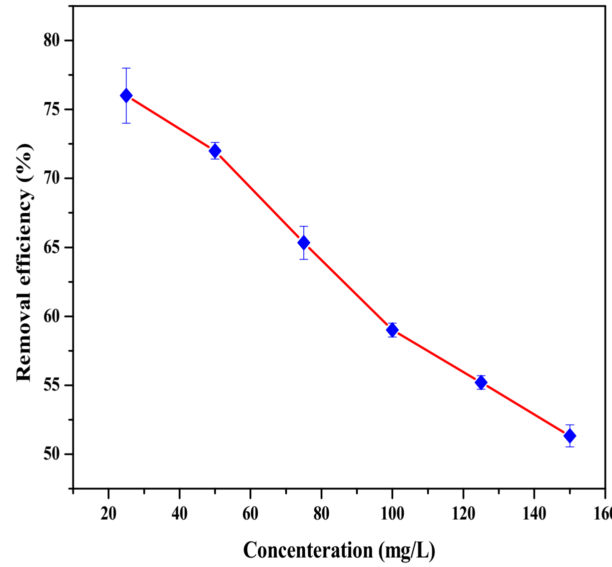

Figure 9. Effect of initial concentration of pesticide on removal efficiency.

3.3 *Adsorption isotherm and kinetics*

Adsorption isotherms are important in depicting the interaction between adsorbate and adsorbent. Figure 10 (a) exhibits the non-linear Langmuir and Freundlich plots for the adsorption of chlorpyrifos on HKUST-1, and various constants obtained from these plots are provided in Table S2 (SI). A higher value of R^2 (0.994) for Langmuir isotherm indicated that a typical Langmuir behavior was observed, relating to monolayer adsorption of chlorpyrifos on independent binding sites of HKUST-1.[24]

In order to get information about the adsorption mechanism, Pseudo first and second-order models were used, where kinetic parameters were calculated (Table S3, SI). The adsorption kinetics at different temperatures, i.e., 30, 45, and 60 °C exhibited an increase in adsorption with the increase in temperature. Figure 10 (b) indicated that the experimental data were best fitted to the pseudo-second-order model. The kinetic parameters also showed that the calculated and experimental values of q_e were closer in PSO, and the value of the coefficient of correlation was more in PSO. It can be concluded from here that the adsorption

Table 1. Comparison of removal efficiency of different organic pollutants using HKUST-1.

Adsorbent	Organic Pollutant	Adsorptive Capacity (mg/g)	Removal Percent (%)	Reference No.
HKUST-1@5% UiO-66	Methylene Blue	526	-	26
HKUST-1	5 % Aqueous Humic Acid	14.42	99	27
HKUST-1	Methylene Blue	750	-	28
HKUST-1	p-nitrophenol	400	-	29
Sulfamic acid@HKUST-1	Malachite Green	290	92	22
Co-ferrite@ HKUST-1	Methyl orange	-	93	30
	Methylene blue	-	97	
AC–HKUST-1	Crystal Violet	133.33	99.76	31
	Disulfine blue	129.87	91.10	
	Quinoline yellow	65.37	90.75	
HKUST-1	Methylene Blue	-	93.57	32
	Reactive Black 5	-	75.01	
HKUST-1	Chlorpyrifos	102	76	This study

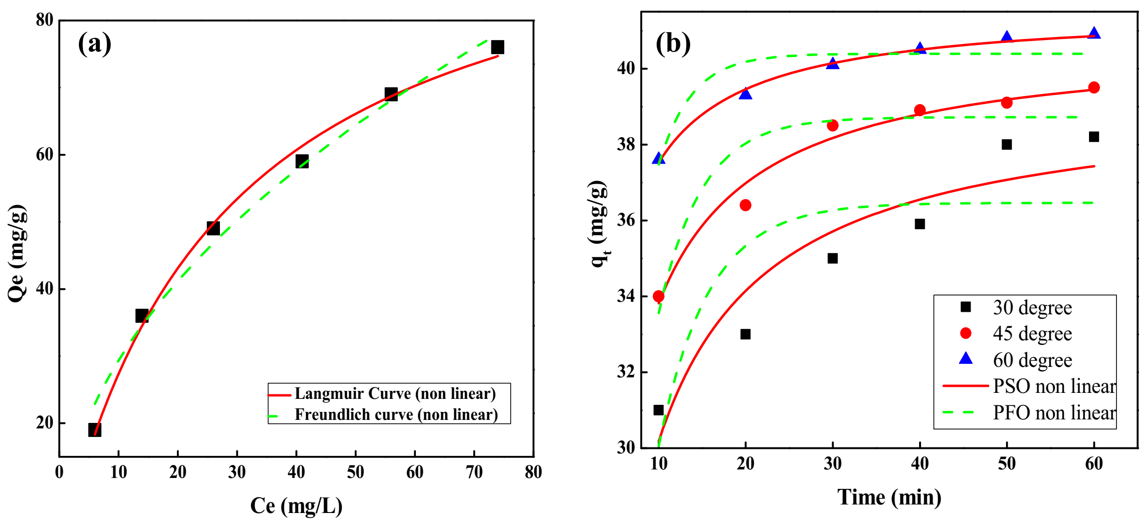

Figure 10. (a) Langmuir and Freundlich isotherm (b) Kinetics: Pseudo first order (dash lines) pseudo second order (solid lines) at 30, 45 and 60 °C.

rate was controlled by chemical interaction between chlorpyrifos and HKUST-1.[25]

4. Conclusions

HKUST-1 was synthesized by a hydrothermal method in this study, and the physicochemical properties were studied by FTIR, XRD, PSA, N_2-sorption, and FE-SEM. Characterization results indicated the successful synthesis of HKUST-1 with octahedral morphology and particle size of 5 µm. HKUST-1 was utilized as an adsorbent for the removal of chlorpyrifos. The maximum removal efficiency of 76% was obtained at pH 7, 20 mg HKUST-1, 30 °C, and 60 min. The maximum adsorptive capacity was reached upto 102 mg/g, probably due to the appreciable surface area and pore volume of the HKUST-1. The highest removal efficiency observed at neutral pH was found to be related to the existence of opposite charges on HKUST-1 and chlorpyrifos surfaces. The data was found to be best fitted for kinetic models of pseudo-second-order and Langmuir adsorption isotherm, which shows that the adsorption process was directed by chemisorption. Thus the use of HKUST-1 was found as an efficient way to remove organophosphate pesticide from the aqueous solution.

Supplementary Information (SI)

Additional information on FTIR, EDX, Pore size distribution, Zeta potential analysis, Isotherm, and Kinetics are available at http://www.ias.ac.in/chemsci.

Acknowledgements

The author thanks Residue Analysis Lab, College of Agriculture, CCSHAU, Hisar, for providing chlorpyrifos; Centre for Bio-Nano Technology, CCSHAU, Hisar, and Indian Institute of Technology Roorkee for help in characterization.

References

1. Mohanadas D, Zainudin N I A and Sulaiman Y 2022 A copper-based metal-organic framework/tungsten trioxide with improved coloration efficiency for electrochromic application *Chem. Eng. J.* **428** 130989
2. Li J R, Sculley J and Zhou H C 2012 Metal–organic frameworks for separations *Chem. Rev.* **112** 869
3. Yepez R, García S, Schachat P, Sánchez-Sánchez M, González-Estefan J H, González-Zamora E and Aguilar-Pliego J 2015 Catalytic activity of HKUST-1 in the oxidation of trans-ferulic acid to vanillin *New J. Chem.* **39** 5112
4. Mallakpour S, Nikkhoo E and Hussain C M 2022 Application of MOF materials as drug delivery systems for cancer therapy and dermal treatment *Coord. Chem. Rev.* **451** 214262
5. Falcaro P, Ricco R, Yazdi A, Imaz I, Furukawa S, Maspoch D, et al. 2016 Application of metal and metal oxide nanoparticles@MOFs *Coord. Chem. Rev.* **307** 237
6. Nabi S, Sofi F A, Rashid N, Ingole P P and Bhat M A 2022 Metal-organic framework functionalized sulphur doped graphene: a promising platform for selective and sensitive electrochemical sensing of acetaminophen, dopamine and H_2O_2 *New J. Chem.* **46** 1588
7. Mahmood I, Imadi S R, Shazadi K, Gul A and Hakeem K R 2016 Effects of pesticides on environment In *Plant, soil and microbes* (Springer: Cham) pp. 253-269
8. Schreinemachers P, Grovermann C, Praneetvatakul S, Heng P, Nguyen T T L, Buntong B, et al. 2020 How much is too much? Quantifying pesticide overuse in vegetable production in Southeast Asia *J. Clean. Prod.* **244** 118738
9. Singh B, Awasthi A and Singh D P 2021 Effects of pesticides on environment and human health *Int. J. Mod. Agri.* **10** 4089
10. Mathur H B, Johnson S and Mishra R 2003 In *Analysis of pesticide residues in bottled water* (Delhi Region). CSE Report.
11. Agrawal A, Pandey R S and Sharma B 2010 Water pollution with special reference to pesticide contamination in India *J. Water Res. Protect.* **2** 1793
12. Rashid R, Shafiq I, Akhter P, Iqbal M J and Hussain M 2021 A state-of-the-art review on wastewater treatment techniques: the effectiveness of adsorption method *Environ. Sci. Pollut. Res.* **28** 9050
13. Diercks C S and Yaghi O M 2017 The atom, the molecule, and the covalent organic framework *Science* **355** 6328
14. Azhar M R, Abid H R, Sun H, Periasamy V, Tadé M O and Wang S 2016 Excellent performance of copper based metal organic framework in adsorptive removal of toxic sulfonamide antibiotics from wastewater *J. Colloid Interface Sci.* **478** 344
15. Zhang Q, Yu J, Cai J, Song R, Cui Y, Yang Y, et al. 2014 A porous metal-organic framework with –COOH groups for highly efficient pollutant removal *Chem. Commun.* **50** 14455
16. Clogston J D and Patri A K 2011 Zeta potential measurement. In *Characterization of Nanoparticles Intended for Drug Delivery* (Humana Press) pp. 63-70
17. Denning S, Majid A A, Lucero J M, Crawford J M, Carreon M A and Koh C A 2020 Metal-Organic Framework HKUST-1 Promotes Methane Hydrate Formation for Improved Gas Storage Capacity *ACS Appl. Mater. Interf.* **12** 53510
18. Chuah C Y, Goh K and Bae T H 2017 Hierarchically structured HKUST-1 nanocrystals for enhanced SF6 capture and recovery *J. Phys. Chem. C* **121** 6748
19. Qian X, Yadian B, Wu R, Long Y, Zhou K, Zhu B and Huang Y 2013 Structure stability of metal-organic framework MIL-53 (Al) in aqueous solutions *Int. J. Hydrogen Energy* **38** 16710
20. Nimbalkar M N and Bhat B R 2021 Simultaneous adsorption of methylene blue and heavy metals from water using Zr-MOF having free carboxylic group *J. Environ. Chem. Eng.* **9** 106216
21. El-Sharkawy R M, Allam E A, Ali A S M and Mahmoud M E 2022 Adsorption study of bisphenol-A and chlorpyrifos onto nanobentonite intercalated with magnetite and sodium alginate: kinetics and isotherm models *Int. J. Environ. Sci. Technol.* **159** 1
22. Kaid M M, Gebreil A, El-Hakam S A, Ahmed A I and Ibrahim A A 2020 Sulfamic acid incorporated HKUST-1: a highly active catalyst and efficient adsorbent *RSC Adv.* **10** 15586
23. Maleki A, Hayati B, Naghizadeh M and Joo S W 2015 Adsorption of hexavalent chromium by metal organic frameworks from aqueous solution *J. Indust. Eng. Chem.* **28** 211
24. Yusuff A S, Popoola L T and Babatunde E O 2019 Adsorption of cadmium ion from aqueous solutions by copper-based metal organic framework: equilibrium modeling and kinetic studies *Appl. Water Sci.* **9** 106
25. Abhari P S, Manteghi F and Tehrani Z 2020 Adsorption of lead ions by a green AC/HKUST-1 nanocomposite *Nanomaterials* **10** 1647
26. Azhar M R, Abid H R, Sun H, Periasamy V, Tadé M O and Wang S 2017 One-pot synthesis of binary metal organic frameworks (HKUST-1 and UiO-66) for enhanced adsorptive removal of water contaminants *J. Colloid Interf. Sci.* **490** 685
27. Ma X, Wang L, Wang H, Deng J, Song Y, Li Q and Dietrich A M 2022 Insights into metal-organic frameworks HKUST-1 adsorption performance for natural organic matter removal from aqueous solution *J. Hazard. Mater.* **424** 126918
28. Kubo M, Moriyama R and Shimada M 2019 Facile fabrication of HKUST-1 nanocomposites incorporating Fe_3O_4 and TiO_2 nanoparticles by a spray-

assisted synthetic process and their dye adsorption performances *Micropor. Mesopor. Mater.* **280** 227
29. Lin K Y A and Hsieh Y T 2015 Copper-based metal organic framework (MOF), HKUST-1, as an efficient adsorbent to remove p-nitrophenol from water *J. Taiwan Inst. Chem. Eng.* **50** 223
30. Saemian T, Gharagozlou M, Hossaini Sadr M and Naghibi S 2020 A comparative study on the pollutant removal efficiency of $CoFe_2O_4$@ HKUST-1 MOF and $CoFe_2O_4$ nanoparticles *J. Inorg. Organomet. Polym. Mater.* **30** 2347
31. Azad F N, Ghaedi M, Dashtian K, Hajati S and Pezeshkpour V 2016 Ultrasonically assisted hydrothermal synthesis of activated carbon–HKUST-1-MOF hybrid for efficient simultaneous ultrasound-assisted removal of ternary organic dyes and antibacterial investigation: Taguchi optimization *Ultrason. Sonochem.* **31** 383
32. Loera-Serna S, Solis H, Ortiz E, Martínez-Hernandéz A L and Noreña L 2017 Elimination of methylene blue and reactive black 5 from aqueous solution using HKUST-1 *Int. J. Environ. Sci. Dev.* **8** 241